

Susceptibility to Stress Corrosion Cracking in Hydrogen Sulfide Environment of MAG Welded Joints of API 5L x 65M Thermomechanical Treated Steel

ION MITELEA, DINU SIMIONESCU, ILARE BORDEASU*
Polytechnica University of Timisoara, 2 Victoriei Sq., 300006, Timisoara

The paper analyzes the stress corrosion cracking behavior of welded MAG welds in pulsed current of thermomechanical treated API 5L X65M. The results of the corrosion tests in hydrogen sulfide (H₂S) environment corroborated with those of the metallographic investigations showed that for the welding conditions established, the pH values and H₂S concentration correspond to the international standards imposed, and the metallic continuity defects are absent.

Keywords: stress corrosion cracking, welded joints, low alloy steel.

Stress corrosion cracking occurs through the simultaneous action of a chemical environment and a static stress regime with at least a tensile effort and which leads to the intergranular or transgranular cracking of the material subjected simultaneously to the two types of actions [1-8]. The onset of this phenomenon in hydrogen sulfide environment causes the metal material to be brittle by hydrogen atoms produced by acid corrosion in the surface area. The absorbed hydrogen is accelerated by the presence of sulfides, hence the fact that the sulfur content of the materials must be strictly controlled. Hydrogen atoms can diffuse into the metallic material, reducing the ductility and toughness characteristics and increasing the susceptibility to cracking [9, 10].

According to the standard API 5L: 2018, for materials used in hydrogen sulfide environment and implicitly in stress corrosion cracking in H₂S environment, their chemical composition is limited to much stricter values [9, 11] than for materials used in normal conditions. Also, according to standard NACE MR0175 / ISO 15156-2: 2015 the hardness of the base metal, the welds and the thermally affected area is limited to 250 HV10 for the inner part of the pipe which is in contact with the corrosive environment, respectively to 275 HV10 for the exterior part that is not exposed to corrosive environment. The filler materials used for welding of materials subjected to stress corrosion cracking in H₂S medium according to NACE MR0175 / ISO 15156-2: 2015 have a content of Ni ≤ 1% [12].

In this paper, investigations are made on the resistance to stress corrosion cracking of welded joints of a thermomechanical treated steel intended for the execution of underground and submarine pipe lines having a diameter of 42 "(1066.8 mm) and a wall thickness of 31.75 mm, the medium corrosive used being hydrogen sulfide (H₂S). This is the most common corrosive environment encountered in the oil and gas transportation.

Experimental part

The welding of the pipelines for the transport of oil and gas has been done by the MAG process in spray arc for the root & hot pass layer and pulsed current for the filling of the joint [13].

Stress corrosion cracking tests were performed under conditions of constant strain, materialized by means of bending pre-stressing devices under a certain angle. The specimens are of a flat strip type with welding perpendicular to the forces acting on them. The stress-strain combination is in the elastic field.

The test consists of applying a bending stress and exposing it to the test environment.

The stress method used was the four-point loaded specimen, after which the maximum deflection (y) is obtained by applying two symmetrical forces at distance H (fig. 1).

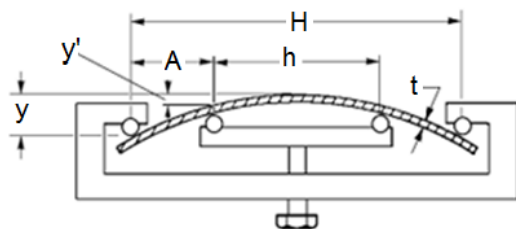


Fig.1 Four point loaded specimen holder
H - distance between outer supports; H = 100 mm
A - distance between inner and outer supports; A = 25 mm;
t - thickness of the specimen; t = 5 mm
h - distance between inner supports; h = 50 mm
y - maximum deflection between outer supports;
y = 0.982 mm; y' - deflection between inner supports;
y' = 0.267 mm

*email: ilarica59@gmail.com, ilare.bordeasu@upt.ro, Phone: 0723650248

The dimensions of the test specimen are shown in fig. 2, and fig. 3 shows the aspect of the specimen before the deformation.

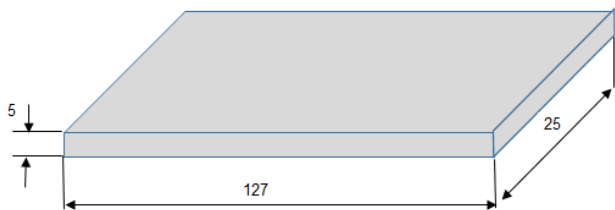


Fig.2 Shape and dimensions of the specimen



Fig.3 Aspect of specimen before deformation

The location of the specimens from welded joints are shown in fig.4.

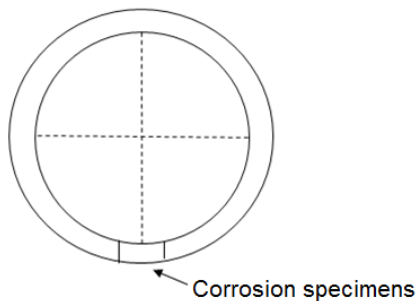


Fig.4 Stress cracking corrosion specimen location

According to figure 5, the specimens were extracted from the root zone, the middle area and the upper part of the welded joint. In total, 12 samples were tested, 4 of each characteristic area of the welded joint.

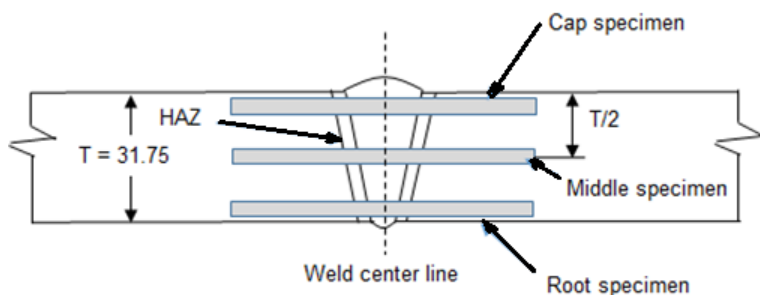


Fig.5 Specimen locations on welded joint section

After cutting, the specimens were machine by milling and wet grinding to obtain a flat surface, then they were polished with emery paper of 120 to 600 grits and finally the surface was cleaned with a solvent (acetone).

Prepared specimens were subjected to 4-point bending stress at a value of the stress level equal to the minimum value of the yield strength of the basic material, 450N / mm². The maximum deflection between outer supports (y) was calculated using the relationship (1), according to the norm ASTM G39:2011:

$$y = \sigma (3H^2 - 4A^2)/12Et = 0.982 \text{ mm} \quad (1),$$

where:

- E – modulus of elasticity = 210 000 N/mm²;
- t – thickness of specimen = 5 mm;
- σ- maximum tensile stress = 450 N/mm²;

H – distance between outer supports = 100 mm;
A – distance between inner and outer supports = 25 mm.

The maximum stress of the specimens is produced between the contact points with the inner supports and is uniform distributed.

The measurement of the maximum deflection, $y = 0.982$, in the central area of the specimen was made by means of a dial indicator (fig. 6).



Fig.6 Measurement of bending specimens

After obtaining the calculated value of the maximum deflection, $y = 0.982$ mm, the inner rollers (central) are blocked so that the deflection will remain constant.

The rollers (outer and inner), made of silicone, are insulators between the test specimen and the bend rig. The schematic diagram of the test installation is shown in figure 7 and its image is shown in fig.8.

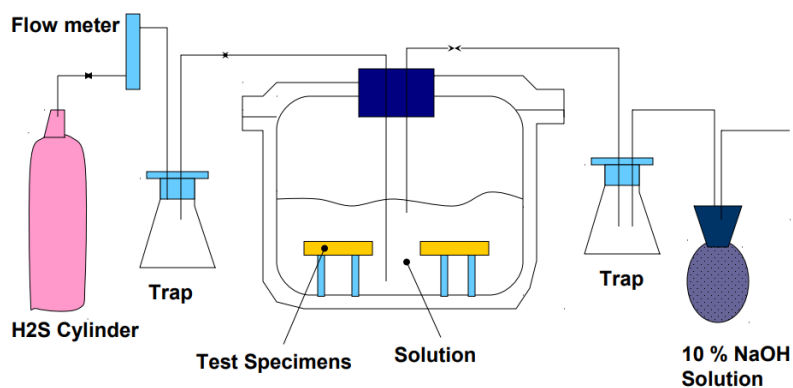


Fig.7. Schematic test installation



Fig. 8. Stress corrosion cracking installation

The specimens constantly strained with the deflection of 0.982 mm are introduced into the glass container, which contains the test solution A according to NACE TM-0177: 2016.

This is an aqueous solution saturated with hydrogen sulfide (H₂S) and consists of 5.0 % weight sodium chloride and 0.5 % weight acetic acid dissolved in distilled water.

The pH value of the prepared solution was, pH = 2.69, and after the purging with nitrogen, the pH became 2.86.

After purging with nitrogen (for oxygen removal) saturation with H₂S takes place over a minimum of 20 min / L of test solution. The value of H₂S concentration after saturation was 2725 ppm. The hydrogen sulfide, H₂S, from the glass container will be refilled periodically three times a week for the duration of the test. The pH and H₂S concentration were measured weekly and at the end of the test.

The values recorded at the end of the test are presented in table 1.

Table 1
VALUES RECORDED

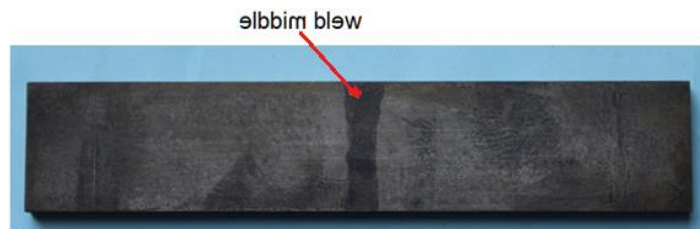
pH/H ₂ S	End of test values
pH	3.62
H ₂ S	3202 ppm

According to NACE TM 0177: 2016, the maximum pH value at the end of the test is 4. The test duration was 720 hours, and the temperature was maintained constant at 24°C ±3°C.

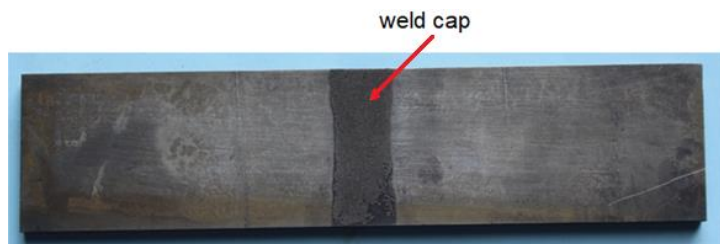
After the test, the bent specimens were removed from the glass container and cleaned with water, detergent and acetone. In Figure 9 a, b and c are shown images of specimens (root, the middle and the top) at the end of the corrosion test.



-a-



-b-



-c-

Fig.9. The appearance of the specimens at the completion of the corrosion test: a – weld root; b – weld middle; c- weld cap

In addition, the international standard NACE TM-0177: 2016, provides the examination under the optical microscope at a 10X magnification of the surface of the tested specimens (fig.10 a, b and c). From the analysis of these images it can be seen that there are no metallic continuity defects, so that the welded joints of the thermomechanical treated steel are not sensitive to the phenomenon of stress corrosion cracking.

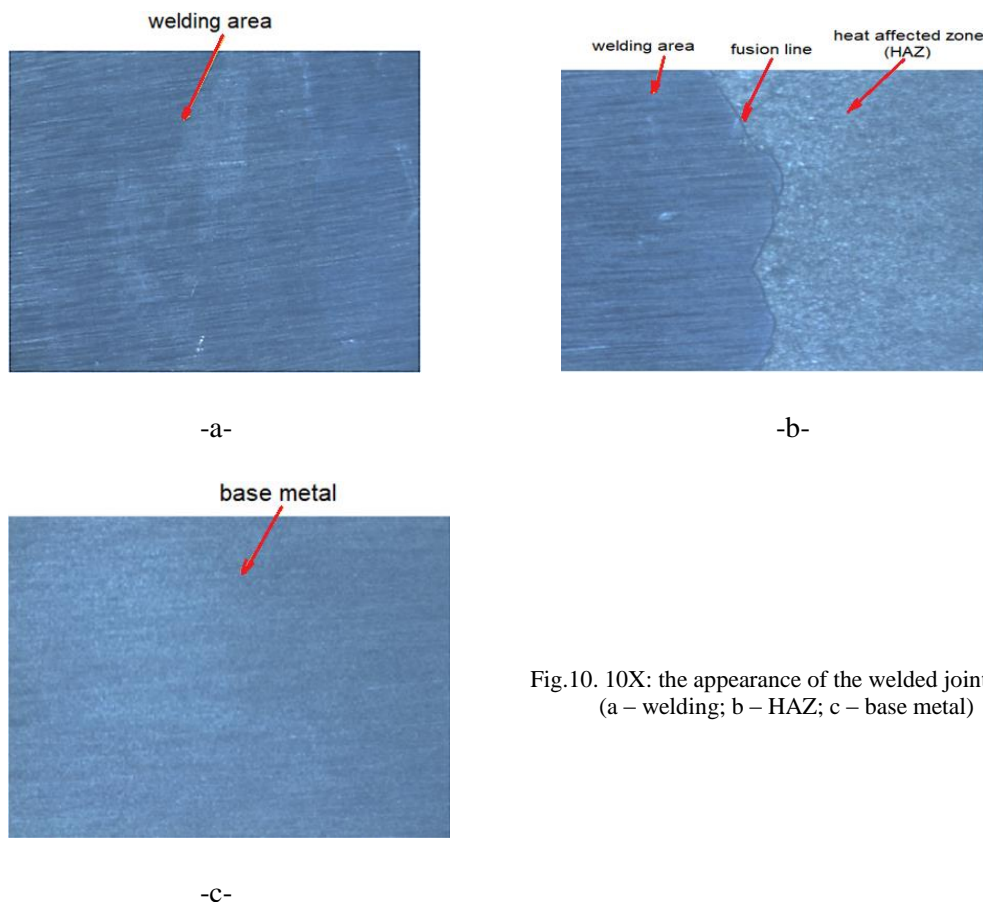


Fig.10. 10X: the appearance of the welded joint areas
(a – welding; b – HAZ; c – base metal)

Conclusions

The selected filler mater and the technological parameters used for the MAG welding in pulsed current demonstrated that the welded joints of the API 5L X65M base material provide a high resistance to stress corrosion cracking in hydrogen sulfide medium.

The specimens subjected to stress corrosion cracking in hydrogen sulfide medium have a pH value of 3.62 with a H₂S concentration equal to 3202 ppm and no cracks were observed in the three welded joint areas.

References

1. STROBL S., Stress Corrosion Cracking, *Pract. Metallogr.* Vol.54, Issue 3, 2017, pp. 153 – 162
2. MELCHERS, E.R., PAIK, K.J., Effect of tensile strain on the rate of marine corrosion of steel plates. *Corrosion Science*, Vol. 52, Issue 10, 2009, pp. 2298 – 2303
3. WINZER, N., ATRENS, A., SONG, G., GHALI, E., DIETZEL, W., KAINER K.U., HORT, N., BLAWERT, C., A critical review of the stress corrosion cracking (SCC) of magnesium alloys. *Adv. Eng. Mater.*, Issue 7, 2005, pp. 659–693
4. BORDEASU, I., POPOVICIU, M.O., MITELEA, I., BALASOIU, V., GHIBAN, B., TUCU, D., Chemical and mechanical aspects of the cavitation phenomena. *Rev. Chim (Bucharest)*, **58**, no. 12, 2007, pp. 1300-1304
5. MITELEA, I., BORDEASU, I., POPOVICIU, M.O., HADAR, A., Corrosion of stainless steels with "soft" martensitic structure, *Rev. Chim (Bucharest)*, **58**, no. 2, 2007, pp. 254-257
6. BURDUHOS-NERGIS, D.P., CARMEN NEJNERU, C., BURDUHOS-NERGIS, D.D., SAVIN, C., SANDU, V.S., TOMA, S.L., BEJINARIU, C., The Galvanic Corrosion Behavior of Phosphated Carbon Steel Used at Carabiners Manufacturing, *Rev. Chim (Bucharest)*, **70**, no.1, 2019, p. 215-219
7. DOBROTA, D., Corrosion of Welded Metal Structures of Mining Equipment, *Rev. Chim (Bucharest)*, **69**, no.9, 2018, p. 2563-2566
8. LUPESCU, S., CORNELIU MUNTEANU, C., ISTRATE, EARAR, K., The Influence of Zr on Microstructure, Mechanical Properties and Corrosion Resistance in Mg-Y-Zr Biodegradable Alloys, *Rev. Chim (Bucharest)*, **69**, no. 12, 2018, p. 3382-3385
9. KANNAN, M.B., DIETZEL, W., Pitting-induced hydrogen embrittlement of magnesium-aluminium alloy. *Mater. Des.* 2012, Vol. 42, pp. 321–326
10. RALSTON, K.D., WILLIAMS G., BIRBILIS, N., Effect of pH on the grain size dependence of magnesium corrosion. *Corrosion*, **68**, 2012, p. 507–517
10. JAFARI, S., HARANDI S.E., SINGH RAMAN R.K., A Review of stress-corrosion cracking and corrosion fatigue of magnesium alloys for biodegradable implant applications. *J. Mater.* Vol. 67, 2015, pp. 1143–1153
11. GARCIA K.E., MORALES A.L., BARRERO C.A., GRENECHE J.M., New contributions to the understanding of rust layer formation in steels exposed to a total immersion test, *Corrosion Science*, Vol.48, 2006, pp. 2813 – 2830
12. SIMIONESCU, D., MITELEA, I., BURCĂ M., Opportunities of narrow gap MAG welding of API 5L X65M steel pipeline. *METAL 2017*, International Conference on Metallurgy and Materials, 2017, pp. 699 – 704

